RSC Advances

This is an *Accepted Manuscript*, which has been through the Royal Society of Chemistry peer review process and has been accepted for publication.

Accepted Manuscripts are published online shortly after acceptance, before technical editing, formatting and proof reading. Using this free service, authors can make their results available to the community, in citable form, before we publish the edited article. This *Accepted Manuscript* will be replaced by the edited, formatted and paginated article as soon as this is available.

You can find more information about *Accepted Manuscripts* in the **Information for Authors**.

ROYAL SOCIETY OF CHEMISTRY

www.rsc.org/advances

Journal Name

ARTICLE

Hybrid Magnetic-Plasmonic Nanocomposite: Embedding Cobalt Cluster *in-situ* Gold Nanorods

A. N. Emam,[a,b] M. B. Mohamed,[c,d]† E. Girgis,[a,e] and K.V. Rao[f]

We developed a method to fabricate hybrid magnetic-plasmonic nanorods (Au-Co NRs) via modified seeded mediated method. The only modification is to use cobalt ions instead of Au^{+3} in the preparation of the seed solution to obtain gold nanorods doped with Co clusters. By adjusting the amount of cobalt seed solution, Au-Co NRs of controlled aspect ratio can be obtained. The optical properties of the obtained Au-Co NRs were investigated and compared to that of the pure Au NRs. Slight shift and broadening were observed in the alloys compared to the pure ones, which attributed to the presence of Co clusters leading to suppression of the dielectric properties. High resolution transmission electron microscopy (HRTEM) images indicate the existence of Co clusters *in-situ* Au NRs host and clearly show the metal-metal interface. The magnetic properties of the obtained Au-Co NRs increases as the concentration of dopant Co clusters seeds increases, as investigated by vibrating sample magnetometer (VSM). Our approach allows us to design nanomaterials of controlled shape, optical and magnetic properties which have many promising applications in tharanostics and photoelectronics.

1. Introduction

Hybrid nanostructures containing both magnetic and another functional phase have been attracting much interest from several researchers due to many important scientific and technological aspects.[1] It is known that plasmonic nanostructures have unusual and pronounced optical properties; where the position of the localized surface plasmon resonance (LSPR) is strongly depends on the particle shape, size, and chemical composition, as well as on the dielectric properties of the surrounding media.[2-22] Thus, LSPR opened many opportunities to be used in a wide range of applications [13,23] including chemical and biological sensing,[24-27] probing,[28] therapy and imaging.[29-38]

Embedding magnetic clusters into plasmonic nanostructures (i.e. Au or Ag nanoparticles) would influence their magnetic and optical properties. In addition, these hybrid nanostructures have magneto-optical (MO) behaviour through the combination between ferromagnetic materials, and LSPR of the plasmonic nanoparticles. This is desirable for developing active nano-plasmonic devices such as magnetic field sensors and data storage.[39]

Their magnetic properties can be controlled via incorporation of ferromagnetic clusters within noble plasmonic nanostructure via chemical route.[40-47] Wang *et al.* synthesized CoPt rod-like nanoalloy via ionic liquid method.[48] Also, Cu-Pt nanorods of controlled aspect ratio had been prepared using a mixture of oleic acid and oleylamine.[49]

Several attempts had been carried out to prepare Au-Co hybrid nanostructure.[50-64] Hall *et al.* focused on a template fabrication of Co/Au core-shell nanorods partially embedded in polycarbonate track-etch, and anodic aluminium oxide nano-porous membranes.[58] Wetz *et al.*[59] studied the parameters affecting the nucleation of Au nanoparticles (Au NPs) on the Co nanorods. Watts *et al.* determined the optimum conditions to grow gold on the surface of Co nanorods by galvanic displacement [60] or by heterogeneous growth.[59] Another structure of cobalt gold hybrid nanostructure was fabricated through formation of thin-film made of Au/Co/Au trilayers via several techniques such as lithography,[50,65] ion beam etching,[47] magnetron sputtering,[61-64] and molecular beam epitaxy (MBE).[64]

In this work, we developed a convenient method to fabricate a rod-like Au-Co hybrid nanocomposite of controlled composition and aspect ratio *via* chemical routes based on seed mediated method.[66,67]

2. Experimental

2.1. Materials

Hydrogen tetrachloroaurate (III) trihydrate ($HAuCl_4.3H_2O$, Aldrich, 99.999%), cobalt acetate ($Co(CH_3COO)_2$, WINLAB, 98%), sodium

borohydride (NaBH$_4$, WINLAB, 98%), N-Cetyl-N,N,N,-Trimethyl-ammonium bromide (CTAB, Merck, 99%), Silver nitrate (AgNO$_3$, Sigma Aldrich, 99%), L-ascorbic acid (Vitamin C, Fluka, 99%) and purified water from the Millipore Milli-Q water purification system.

2.2. Shape controlled synthesis of bimetallic Au-Co hybrid nanostructure

Colloidal Au-Co NRs has been prepared via seed-mediated method as described previously[66,67] with little modification to introduce Co^{2+} ions *in-situ* the lattice of the gold nanorods. Cobalt precursor was used instead of gold within the seed solution to induce the magnetic impurities as a dopant. In typical method; CTAB-stabilized seed solution of cobalt nanoclusters was prepared by reduction of 5.0x10^{-3}M Co(CH$_3$COO)$_2$ and 0.2 M CTAB with ice-cold aqueous 0.01 M NaBH$_4$. 5 ml of an aqueous growth solution containing 0.2 M CTAB, 70 µl of 4x10^{-3}M AgNO$_3$ and 1x10^{-3}M HAuCl$_4$.3H$_2$O in a test tube. Addition of the CTAB produced a colour change from yellow to brown-yellow suggesting the existence of ligand-substituted anions such as CTAB–Au^{+3} complex. Then 50 µl of 0.1M L-ascorbic acid was added and followed by addition of specific volume of the seed solution. The colour of the solution gradually changed indicating the growth of the gold nanorods. The prepared particles have been separated from the growth solution to remove the excess CTAB by centrifugation at 10°C.

2.3. Characterization

UV-Visible absorption spectra for the prepared samples have been recorded using Ocean Optics USB 2000 spectrometer. The absorption was recorded within the appropriate scan range from 190 to 1100 nm. High Resolution Transmission Electron Microscope (HRTEM) model JEM-2100, equipped with scanning image observation device to give bright and dark-field STEM images at 200 kV, was used to investigate particle size, shape, and the chemical composition of the obtained samples. The unit comprises energy dispersive X-ray analyzer model JED-2300T. The XRD was recorded using Panalytical X'Pert Pro, Cu Kα radiation, λ = 1.546Å) over a 2θ range of 4°-80°. In addition, the exact content of Co^{2+} in-situ the Au rods were performed using atomic absorption spectrometer (AAS) Varian Spectra AA 220/FS. Finally, the magnetic measurements were carried out using vibrating sample magnetometer (VSM), ADE Technologies, Inc. EV11 (Model 8810).

3. Results and discussion

In order to investigate the influence of cobalt *in-situ* gold nanostructure on the optical and magnetic properties, gold and Au-Co nanospheres were prepared. Spherical gold particles prepared by reducing gold ions using NaBH$_4$ in presence of CTAB as a capping material. The same method used to prepare Au-Co spherical hybrid nanostructure, but instead of using gold ions, a mixture of gold and cobalt ions had been used. Figure 1 represents the optical properties and the transmission electron microscopy (TEM) micrographs for the as-prepared particles from pure gold (Au), and gold-cobalt (Au-Co) nanoparticles (NPs). Based on the absorption spectra (Figure 1a), it is clear that the spherical-like shape has been formed for each of pure Au gold particles (black line), and Au-Co nanoalloy (red line). The absorption spectra show only one absorption band, where the maximum wavelength (λ$_{max}$) was about 523 nm owing to its surface plasmon resonance (SPR). The absorption spectrum of the Au-Co alloyed NPs shows a broader absorption red shifted than the plasmon band of the pure Au NPs, where (λ$_{max}$) was about 530 nm, which is in agreement with the commonly observed in other Au bimetallic systems.[68-71]
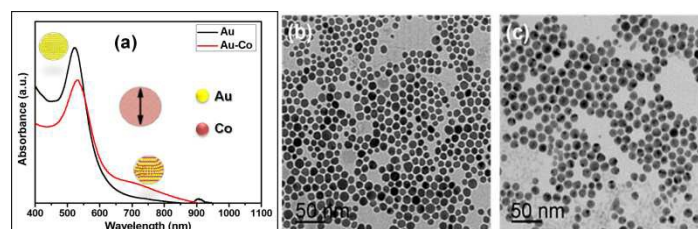

Figure 1. (a) UV-Vis absorption spectrum, TEM images for both of (b) pure Au, and (c) hybrid Au-Co NPs.

This was confirmed by imaging these particles using TEM as shown in Figures 1b and 1c. It is clear that the obtained particles are uniform spherical nanoparticles. In case of Au NPs, the average size (D) was around 12±1.5 nm with size distribution about ~ 5.4% rms (Figure 2b). The average size is about 15±1.5 nm for cobalt doped gold NPs with size distribution about ~ 6.7% rms (Figure 1c). Slight red shift and broadening has been observed in absorption spectrum of Au-Co bimetallic NPs relative to the pure Au NPs. This might be due to the fact that the size distribution of pure Au NPs is narrower than that of the Au-Co NPs, and the aggregation of Au-Co NPs is more serious than the pure Au NPs. Also, the homogenous mixture of metal-metal bond between gold and cobalt leads to formation of

an intermetallic or alloyed structure, where Co clusters diffuses into Au NPs host crystal.[70,72] Templeton *et al*. reported that any change in the pure Au cores causes shift in the Plasmon band.[73] Thus, the electronic properties induced by the presence of cobalt clusters may also affect plasmon band position; as Au character increases and the Co becomes buried beneath the Au, these dielectric effects may be suppressed (Figure 1a).[74-76]

Rod-Shaped Au-Co Nanoalloy: Seed mediated method was used to prepare pure gold nanorods.[66-67] In order to prepare Au-Co nanorods, the cobalt seed solution has been used instead of gold seed solution and added to the growth solution leads to formation of bimetallic gold-cobalt nanorods.

Cobalt nanoclusters (seed solution) were prepared via chemical reduction of cobalt acetate in the presence of cationic surfactant (i.e. CTAB), which act as a capping material. $NaBH_4$ has been used as a reducing agent. The role of acetate (i.e. CH_3COO^-) anion on formation of cobalt seed particles is to stabilize the cobalt nanoclusters similar to citrate ($C_3H_5O(COO)_3^{3-}$) anion role in synthesis of metallic nanoparticles in combination with polymeric surfactant.[77] Moreover, the presence of acetate anion may increase the rate of colloid formation due to its lower redox potential than other anion such as nitrate (NO_3^-), ascorbate, and bromide.[78]

Figure (2) shows TEM and SAED micrographs of the prepared cobalt seed. It is clear that tinny spherical clusters are predominant of average size ~ 5.2±1.5 nm as shown in Figure (2a). The crystallographic structure of individual cobalt clusters shows four reflection planes (400), (101), (110) and (311), which refer to the hexagonal structure of cobalt. The inter-planer distance was about 0.89, 1.92, 1.24, and 1.08Å, respectively.
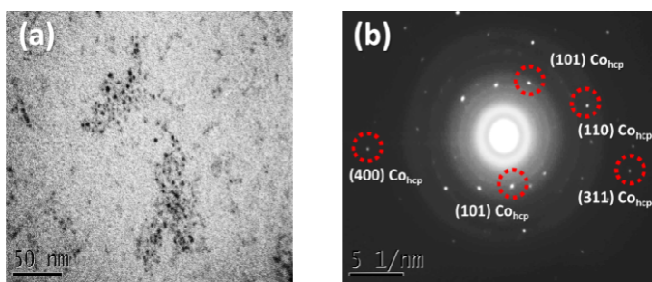

Figure 2. (a) TEM and (b) SAED micrographs of cobalt seeds.

The formation of rod-shaped Au-Co hybrid nanostructure confirmed using absorption spectra and TEM images (see Figure 3). It is well known that anisotropic rod-shaped plasmonic nanostructure is characterized by two modes of surface electrons oscillation, the first one is owing to the transverse surface plasmon resonance (T-SPR), and the other mode is owing to the longitudinal surface plasmon resonance (L-SPR).[17] Figure 3a shows the absorption spectra for pure Au(black line), and Au-Co NRs(red line). The aspect ratio (*R*) of the rod has been calculated from the absorption maximum of the L-SPR using the equation developed by Link *et al*.,[79] where *R* was found to be 3.19 and 3.29 for both of Au-Co and Au NRs, respectively. It is clear that the absorption spectrum of rod shaped gold-cobalt hybrid nanostructure is slightly blue shifted than that of the pure gold nanorods. The T-SPR is blue shifted from 530 nm to 518 nm and the L-SPR band is blue shifted from 733 to 724 nm, for the case of pure gold nanorods and Au-Co hybrid NRs, respectively (Figure 3a). It was reported that the plasmonic absorption depends on the ratio of the constituent materials.[80] Blue shift in the plasmonic absorption of Co-Au nano-alloys has been reported by Xu*et al*.[81] They attributed the blue shift of the plasmonic band to the change of the surface charge density and the mean free path of electron, due to the embedding of cobalt clusters in-situ gold matrix. This leads to loss of the continuous density of states in the gold matrix.[80-82] Figures 3c, and 3d show the high resolution TEM images of the pure gold nanorods and the hybrid Au-Co nanostructure which clearly show the embedding of cobalt clusters in-situ the gold host.
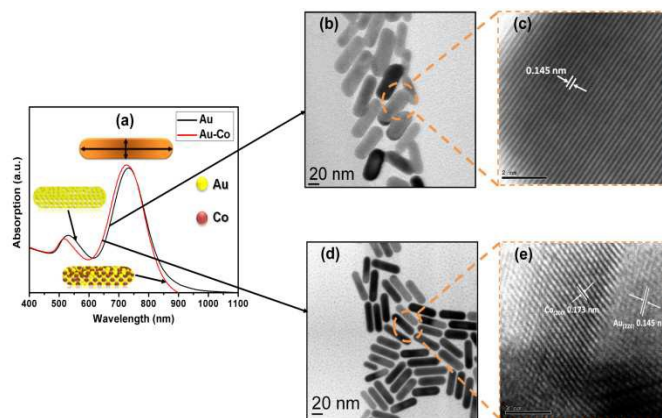

Figure 3. (a) UV-Vis absorption spectrum, TEM images for both of (b) Pure Au, and (d) Au-Co NRs, and HR-TEM lattice image for both of (c) Pure Au, and (e) Au-Co NRs

To investigate the crystal structure and confirm the formation of cobalt nanoclusters *in-situ* Au-Co NRs, selected area electron diffraction (SAED) patterns, HRTEM and XRD were recorded and represented in Figures 4, 5 and 6, respectively. The SAED patterns show that, the diffraction spots are superimposed on the rings indicating the polycrystalline structure of the rod shape. In contrast, Au-Co hybrid nanorods

were obtained by inserting cobalt clusters into gold nanorods. The *d*-spacing of adjunct fringes was found to be 0.126 nm, which is similar to the planar distance of Au[311] (0.123 nm) or Co[110] (0.125 nm). Also, the d-spacing of another adjunct fringes 0.21 nm and 0.089 nm, which similar to the planner distance of Au[200] or Co[400]. Therefore, it is important to understand the role of cobalt cluster in enhancing the growth of rod shape, and inducing the magnetic properties to the gold nanorods.
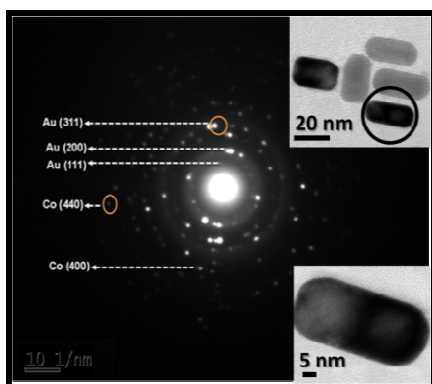

Figure 4. SEAD patterns for prepared Au-Co NRs.

HR-TEM images in Figure 5a shows breaking in the symmetry within the gold crystal lattice, due to the existence and diffusion of cobalt atoms through the gold lattice at the metal-metal interface. The lattice image at seed concentration of $1x10^{-3}$ M (i.e. 11.197µg) shows d-spacing = 0.079 nm and 0.154 nm, which is similar to the planar distance of Au[511] (0.078nm) or Co[102] (0.148nm). While in case of using $5x10^{-4}$ M (i.e. 5.598µg) of cobalt ions, the d-spacing is 0.145 nm and 0.173 nm is similar to the planer distance of Au[220] (0.144nm) or Co[200] (0.178nm) (Figure 5b).
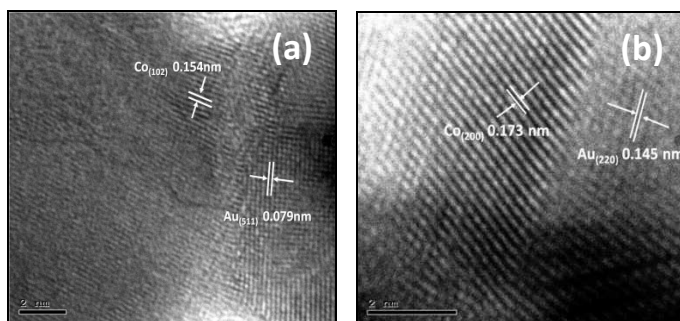

Figure 5. HRTEM micrograph for prepared gold nanorods doped with Co^{2+} ions at fixed concentration Co^{2+} ions of $1x10^{-3}$ M (i.e. 11.197µg) (a), and $5x10^{-4}$ M (i.e. 5.598µg)(b) in seed solution.

Four distinct features at 2θ = 38.2, 44.4, 64.6 and 77.6^O have been observed in the XRD pattern of the Au NRs, which can be assigned to the strongest line reflections from (111), (200), (220) and (311) planes of the face-centered-cubic (fcc) of Au. In case of Au-Co NRs,

three additional peaks appears at 2θ =34.0, 41.8 and 51.03 which attributed to reflections from (211), (213) and (400) plans of hexagonal-closed-packed (hcp) of Co clusters embedded in the gold nanorods.
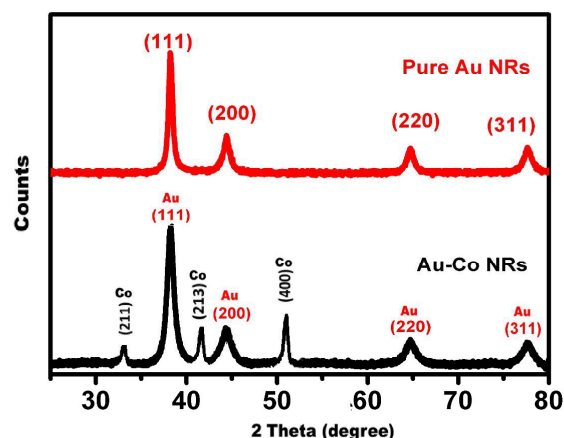

Figure 6. XRD Patterns for the prepared Au-Co nanorods (black) compared to the pure Au NRs (red).

Energy dispersive x-ray (EDX) measurement is a powerful technique, which allows us to determine the exact ratio of elements in-situ the samples during imaging of the rods. Figure 7 represents the EDX data for each of Au and Au-Co NRs, It clear that the cobalt and gold content have an average of about 13.65, and 86.35 wt%, respectively. This is significant indication for the doping and diffusion of Co clusters in the gold nanorods matrix, and the formation of hybrid rod-shaped Au-Co nanostructure. Atomic absorption spectroscopy measurementswere performed to ensure the presence of cobalt in the gold nanorod sample and to confirm EDX results. The exact Co^{2+} content in Au-Co NRs sample as measured by atomic absorption was about 3.762 µg, while the calculated content theoretical was 5.598 µg for $5x10^{-4}$M of Co^{2+} ions seed solution.
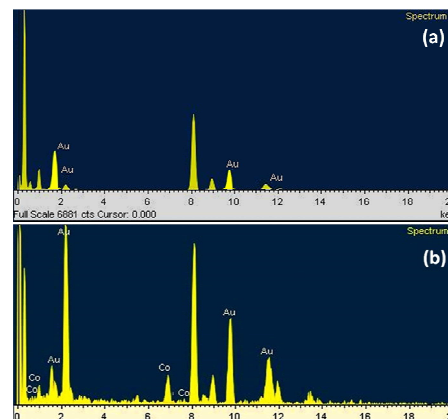

Figure 7. The EDX analysis for both of Pure Au NRs (a), and Au-Co NRs (b)

The size and shape of Au-Co NPs could be tuned by changing the cobalt concentration in the seed solution (Figure 8 and 9). The effect of the cobalt concentration on the growth of gold nanorods was monitored by measuring the absorption spectra and TEM images of the obtained Au-Co NRs prepared using different cobalt ions concentration (i.e. 111.92 to 5.598µg).
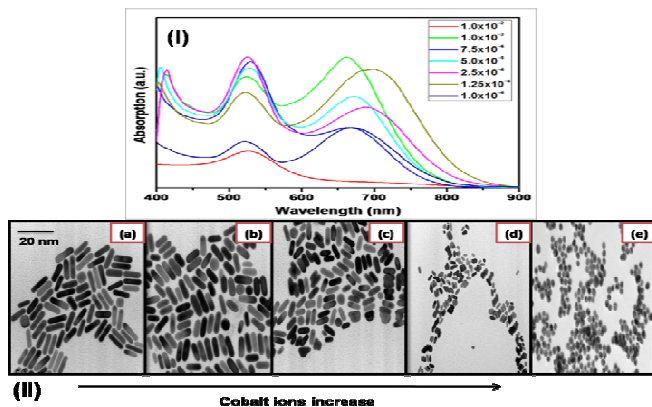

Figure 8. (I) Absorption spectra of the obtained gold nanorods using different molar concentration of Co^{2+} ions in the seed solution varied from 1.0×10^{-4} M to 0.01M. (II) TEM images of the obtained Au-Co hybrid NRs at different Co^{+3} concentrations (a)1.0×10^{-4}M, (b)1.25×10^{-4}M, (c)1.5×10^{-4}M, (d)1.0×10^{-3}M & (e)1.0×10^{-2}M respectively.

To emphasis the effect of the amount of cobalt ions concentration on the growth rate of different facets of gold particles, different amount of the seed (i.e. cobalt clusters) has been used to prepare gold nanorods of different aspect ratios. Our result confirms that introducing small amount of seed lead to formation of longer rods (i.e. aspect ratio ~ 3.0). Increasing the amount of seed, more than 170 µl (i.e. 100.2 µg), leads to formation of spherical shape. Table 1 summarizes the effect of cobalt ions concentration on the final aspect ratio of the Au-Co nanoparticles.The aspect ratio of the gold nanorods have been calculated from the absorption spectra using the equation proposed by Link *et al*.[79]
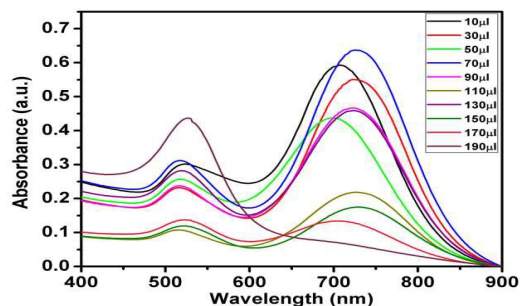

Figure 9. Absorption spectra of prepared gold nanorods doped with Co^{2+} series with various aspect ratios using different amounts seed at fixed concentration Co^{2+} ions in seed (1×10^{-2}M).

It is clear from Table 1 that the aspect ratio of the rod-shaped Au-Co hybrid nanostructure decreases as the concentration of cobalt in the seed solution increases.

Table 1. The effect of the seed concentration on the aspect ratio of the Au-Co nanorods

Seed(µl)[a]	10	30	50	70	90	110	130	150	170	190
Co^{2+} Ions (µg)[b]	5.9	17.7	29.45	41.25	53.04	64.82	76.6	88.4	100	112
R (Cal.)[c]	3.0	3.2	2.9	3.26	3.19	3.21	3.17	3.24	2.98	1.13

[a] Volume of Co^0 seed solution in (µl). [b] Cobalt ions content in seed solution in (µg). [c] Calculated aspect ratio.

To understand the mechanism of formation and growth of gold nanorods doped with magnetic ions (i.e. Co^{2+} ions). It is important to investigate the role of cobalt cluster on the growth of the rod-shaped particles, and the magnetic properties of the Au-Co NRs. According to previous studies on silver-assisted growth of gold nanorods, there are two mechanism has been proposed. The first introduced by Murphy and co-workers,[66] which proposed that AgBr adsorbed into the facets of the gold nanocrystals, which slow down the gold reduction, and induces single crystalline growth of the Nanorods. The other one proposed by Nikoobakht and El-Sayed[67] at which they modified Murphy method and used CTAB-capped seeds rather than citrate-capped ones. They proposed that the surfactant (CTAB) forms a soft template with a certain size that depends on surfactant concentration, pH and ionic strength of the solution.

The proposed growth mechanism in our study based on the galvanic replacement reaction between single-crystal Co nanorods of seed and $AuCl^{-4}$ ions. Due to strong size-dependent of redox potentials of nanomaterials (i.e. Co clusters), where the redox potential of Co^{2+} (~ -0.28 Volt) is lower than Au^{3+} (~ +1.50 Volt) and Ag^{1+} (~ +0.80 Volt). Thus, the cobalt nanoclusters capped with CTAB adsorbed faster on the surface of the gold particle. The adsorbed cobalt atoms, probably forming stable clusters,[77,78] which then act as a catalyst to enhance the growth of the gold nanorods. Gold particles with a cubic lattice have a tendency to grow forming cubes, or spheres, because the rate of the growth of all facets is the same. However, adsorption of cobalt clusters on one of these facets, leads to breaking the symmetry of the growth, and enhance the growth of one of these facets much more than the others. This leads to the formation of rod shaped particles (Scheme 1). This proposed mechanism is agreed with the mechanism reported by Liu and Guyot-Sinnnest.[83]
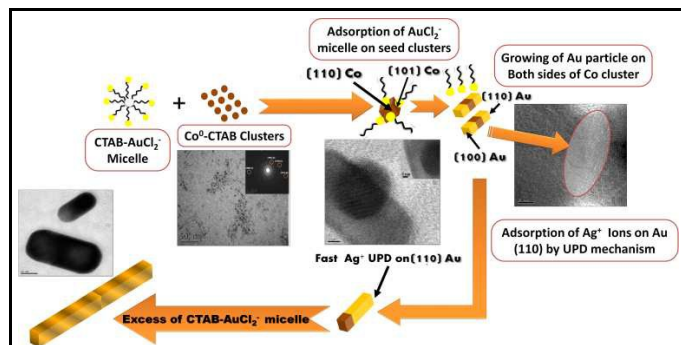
Scheme 1. Shows the proposed mechanism of rod shaped Au-Co hybrid nanostructure

In order to confirm this proposed mechanism, STEM images were recorded for gold nanorods and Au-Co nanorods in order to illustrate the distribution for both of Au, and Co *in-situ* Au-Co nanorods as shown in Figure (10).
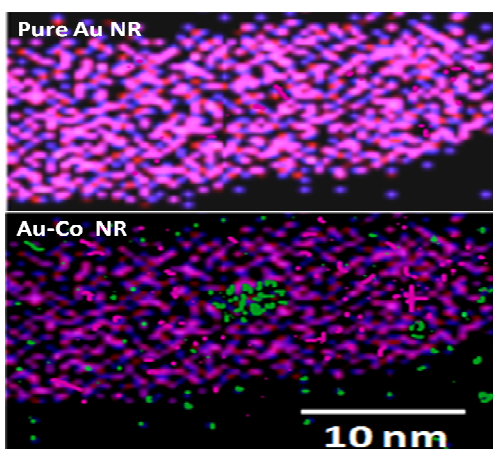

Figure 10. Represents STEM micrograph mapping the distribution for both Au-M (pink square), and Co-K (Green square) in-situ the gold nanorods.

Figure (11) represents the hysteresis loops of Au nanoparticles doped with different concentration of Co^{2+} ions at fixed volume of seed solution, which have been measured using VSM at room temperature (27°C). The hysteresis loop at the highest Co seed concentration (7.5×10^{-4}M) shows a high magnetic moment, and high switching field (Figure 11a). As shown above, increasing the concentration of the Co^{2+} ions leads to increase the doping ions within the Au nanoparticles and formation of spherical particles instead of rods. In addition, due to formation of spherical nanoparticles, the magnetization at the doped magnetic atoms might have no preferred orientation to rotate leading to increase the switching field. As the concentration of the dopants decrease gradually as shown in Figure 11b, it is clear that the hysteresis loop show low magnetic moment and low switching field compared with Figure 11a. This is confirmed by TEM images, which show that Au pasrticles start to form a small ellipse shape (Figure 8II). While in

Figure 11c, it is clear that the magnetic moment is low compared with Figures 11a and 11b due to decreasing the concentration of the Co^{2+} ions. From TEM images, it is clear that by decreasing the doping concentration of the Co^{2+} ions, the Au NPs start to have nanorods shape where the magnetization at the magnetic atoms might be start to have a preferred orientation to rotate leading to decrease the switching field of the nanoparticles. The magnetic moment at Figure 9c is low compared with Figures 11a and 11b, which is due to decreasing the concentration of the Co^{2+} ions and might be due to by forming nanorods, the magnetization of the magnetic atoms has a preferred orientation to rotate. At Figure 11d, it is clear that the magnetic moment and the switching field decreased by decreasing the concentration of the Co^{2+} ions. From TEM images and VSM measurements, it is clear that at very low concentration of Co^{2+} ions, the Au NPs have rods shape, which has a magnetic behaviour with very low switching field and low magnetic moment. These results are very important for magneto-plasmonic and biomedical applications.These hybrid Au-Co nanocomposites present low tendency to be separated using an external magnetic field. This is attributed to the very low content of cobalt in-situ the gold rods. In addition to the presence of the cationic surfactant (i.e. CTAB), which reduce the magnetic behaviour of the obtained nanohybrids.[84,85] The capping agent have a fetal influence to reduce its magnetic properties, even in presence of magnetic dopant (i.e. cobalt Clusters).[86]
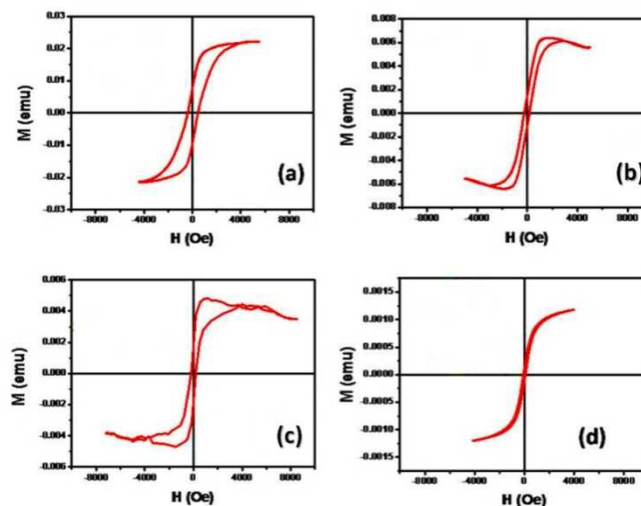

Figure 11. Hysteresis loops of Au nanoparticles with different concentration of Co^{2+} ions (a) 7.5×10^{-4}M, (b) 5×10^{-4}M, (c) 2.5×10^{-4}M and (d) 1.25×10^{-4}M respectively.

4.   Conclusion

Hybrid magneto-plasmonic nanocomposites of controlled shapes (i.e. spheres and rod-like shape) had been prepared. Our method is

based on seeded mediated method at which the magnetic nanoclusters have been used as a seed. We prepared hybrid Au-Co NRs and studied the physical properties of these hybrid nanostructure including optical and magnetic measurements. Our approach allows us to design different hybrid nanomaterials of controlled shape, optical and magnetic properties which has many promising applications in photonics, tharanostics and electronics.

Acknowledgements

Notes and references

[a.] *Advanced Materials & Nanotechnology Lab., Centre of Excellence for Advanced Sciences (CEAS), National Research Centre (NRC), Giza, Egypt.*
[b.] *Biomaterials Department, National Research Centre (NRC), Giza, Egypt.*
[c.] *National Institute of Laser Enhanced Sciences (NILES), Cairo University, Giza, Egypt.*
[d.] *Nanotech Egypt for Photo-electronics, Dream Land City, Giza, Egypt*
[e.] *Solid State Physics Department, National Research Centre (NRC), Giza, Egypt.*
[f.] *Department of Materials Science, Royal Institute of Technology, Stockholm, S-100 44 Sweden*

†**Correspondence**: Dr. Mona B Mohamed monabmohamed@gmail.com

1. Davis, R.,*Powder Technology*. 2001, 119, 45.
2. Kastner, M. A., *Artificial Atoms Physics Today*. 1993, 46, 24.
3. Kreibig, U.; Vollmer, M., Optical Properties of Metal Clusters; Springer: Berlin 1995.
4. Papavassiliou, G. C.,*Prog. Solid State Chem.* 1979, 12, 185.
5. Bohren, C. F.; Huffman, D. R., Absorption and Scattering of Light by Small Particles; Wiley: New York 1983.
6. Creighton, J. A.; Eadon, D. G.,*J. Chem. Soc. Faraday Trans.* 1991, 87, 3881.
7. Mie, G.,*Ann. Phys.* 1908, 25, 377.
8. Mulvaney, P.,*Langmuir* 1996, 12, 788.
9. Gans, R. V.,*Ann. Phys.* 1915, 47, 270
10. Link, S.; El-Sayed, M. A.,*Int. Rev. Phys. Chem.* 2000, 19, 409.
11. Link, S.; El-Sayed, M. A,*Annu. Rev. Phys. Chem.* 2003, 54, 331.
12. Kerker, M.,The Scattering of Light and Other Electromagnetic Rediation; Academic: New York, 1969.
13. Scholl, J. A.; Koh, A. L.; and Dionne, J. A.,*Nature.* 2012, 483, 421.
14. Coronado, E. A.; Encina, E. R.; and Stefani, F. D.,*Nanoscale.* 2011, 3, 4042.
15. Murray, W. A.; and Barnes, W. L.,*Adv. Mater.* 2007, 19, 3771.
16. Halas, N. J., *MRS Bull.* 2005, 30, 362.
17. Angelomé, P. C.; Mezerji, H. H.; Goris, B.; Pastoriza-Santos, I.; Pérez-Juste, J.; Bals, S.; and Liz-Marzán, L. M., *Chem. Mater.* 2012, 24, 1393
18. Juluri, B. K.; Zheng, Y. B.; Ahmed, D.; Jensen, L.; and Huang, T. *J., Chem. C*ommun., 2008, 112, 7309.
19. Rodríguez-González, B.; Attouchi, F.; Cardinal, M. F.; Myroshnychenko, V.; Stéphan, O.; de Abajo, F. J.G.; Liz-Marzán, L. M.; and Kociak, M.,*Langmuir* 2012, 28, 9063
20. Liz-Marzan, L. M..*Langmuir*. 2006, 22, 32
21. Noguez, C.,*J Phys Chem. C* 2007, 111, 3806
22. Lee, K.S.; El-Sayed, M.A.,*J. Phys. Chem. B*. 2006, 110, 19220.
23. Burda, C.; Chen, X.; Narayanan, R.; and El-Sayed, M. A.,*Chem. Rev*. 2005, 105, 1025
24. Jain, P. K.; Huang, X.; El-Sayed, I. H.; El-Sayed, M. A.,*Acc. Chem. Res.* 2008, 41, 1578.
25. Liu, S.; and Tang, Z.,*J. Mater. Chem.* 2010, 20, 24.
26. Willets, K. A.; and Duyne, R. P. V. *Ann. Rev. Phys.Chem*. 2007, 58, 267
27. Haes, A. J.; Stuart, D. A.; and Duyne, R. P. V., Nanotechnology in Biology and Medicine Methods, Devices, and Applications; CRC Press, 2007.
28. Sagle, L. B.; Ruvuna, L. K.; Ruemmele, J. A.; and Van Duyne, R. P. *Nanomedicine.* 2011, 6, 1447.
29. Wang, Z.; Ma. L.,*Coord. Chem. Rev..* 2009, 253, 1607
30. Homan, K. A.; Chen, J.; Schiano, A.; Mohamed, M.B.; Willets, K. A.; Murugesan, S.; Stevenson, K. J.; and Emelianov, S. *Adv. Funct. Mater.* 2011, 21, 1673
31. Wilson, K.; Homan, K.; and Emelianov, S. *Nature Commun.* 2012, 3, 618
32. Homan, K.; Souza, M.; Truby, R.; Luke, G. P.; Green, Vreeland, E.; and Emelianov, S.,*ACS nano.* 2012, 6, 641
33. El-Sayed, I.H.; Huang, X.; El-Sayed, M. A., *Nano Lett*. 2005, 5, 829.
34. Loo, C.A.; Lowery, A.; Halas, N.; West, J.; Drezek, R.,*Nano Lett.* 2005, 5, 709.
35. Haes, A. J.; Van Duyne, R.P.,*J. Am. Chem. Soc.* 2002, 124, 10596.
36. Elghanian, R.; Storhoff, J.J.; Mucic, R. C.; Letsinger, R. L.; Mirkin, C.A.,*Science*. 1997, 277, 1078.
37. Sonnichsen, C.; Reinhard, B. M.; Liphardt, J.; Alivisatos, A.P. *Nature. Biotechnol*. 2005, 23, 741.
38. Hirsch, L.R.; Stafford, R. J.; Bankson, J. A.; Sershen, S. R.; Rivera, B.; Price, R. E.; Hazle, J. D.; Halas, N. J.; West, J. L.,*PNAS.* 2003, 100, 13549.
39. Scott, G. B.; Lacklison, D. E.,*Magnetics IEEE Trans.* on. 1976, 12, 292.
40. Murray, W. A.; and Barnes, W. L.,*Adv. Mater.* 2007, 19, 3771.
41. Hao, E.; Schatz, G. C.,*J. Chem. Phys.* 2004, 120, 357.
42. Sweatlock, L.A.; Maier, S. A.; Atwater, H. A.; Penninkhof, J. J.; Polman, A.,*Phys. Rev. B* 2005, 71, 235408.
43. Schuck, P. J.; Fromm, D. P.; Sundaramurthy, A.; Kino, G.,*Phys. Rev. Lett.* 2005, 94, 017402.
44. Anderson, M. S., *Appl. Phys. Lett.* 2008, 92, 123101.
45. Schatz, G. C.; Van Duyne, R. P. Electromagnetic Mechanism of Surface-enhanced Spectroscopy. In Handbook of Vibrational Spectroscopy. Chalmers, J. M.; Griffiths, P. R., Eds.; Wiley: New York, 2002, pp 759-774.
46. Ozbay, E,.*Science.* 2006, 311, 189
47. González-Díaz, J. B.; García-Martín, A.; García-Martín, J.M.; Cebollada, A.; Armelles, G.; Sepúlveda, B.; Alaverdyan, Y.; and Käll, M.,*Small.*2008, 4, 202.
48. Wang, G.-F; Van Hove, M.A.; Ross, P.N.; Baskes, M.I., *J. Chem. Phys.* 2005, 122, 024706.
49. Wang, C.; Yin, H.; Chan, R.; Peng, S.; Dai, S.; Sun, S.,*Chem. Mater.* 2009, 21, 433.
50. Abe, M.; Suwa, T., *Phys. Rev B.* 2004, 70, 235103.
51. Wu, H.Y.; Choi, C.J.; Cunningham, B.T., *Small.*2012, 8, 2878.

52. Shi, W.; Zeng, H.; Sahoo, Y.; Ohulchanskyy, T. Y.; Ding, Y.; Wang, Z. L.; Swihart, M.; Prasad, P. N.,*NanoLett.* 2006, 6, 875.

53. Carbone, L.; Cozzoli, P.D. *Nano Today.* 2010, 5, 449.

54. Shim, M.; McDaniel, H.,*Current Opinion in Solid State and Materials Science.* 2010, 14, 83.

55. Teranishi, T.; Inoue, Y.; Nakaya, M.; Oumi, Y.; Sano, T.,*J. Am. Chem. Soc.* 2004, 126, 9914.

56. Teranishi, T.; Saruyama, M.; Nakaya, M.; Kanehara, M., *Angew. Chem.* 2007, 119, 1743.

57. Shi, W.; Sahoo, Y.; Zeng, H.; Ding, Y.; Swihart, M. T.; Prasad, P. N., *Adv. Mater.* 2006, 18, 1889

58. Pana, O.; Teodorescu, C.M.; Chauvet, O.; Payen, C.; Macovei, D.; Turcu, R.; Soran, M.L.; Aldea, N.; Barbu, L.,*Surface Science.* 2007, 601, 4352.

59. Wetz, F.; Soulantica, K.; Falqui, A.; Respaud, M.; Snoeck, E.; and Chaudret. B., *Angew. Chem.* 2007, 119, 7209.

60. Poondi, D.; Singh, J., *J. Mater. Sci.* 2000, 35, 2467.

61. Armelles, G.; González-Díaz, J. B.; García-Martín, A.; García-Martín, J. M.; Cebollada, A.; González, M. U.; Acimovic, S.; Cesario, J.; Quidant, R.; and Badenes, G.,*Optics Express* 2008, 16, 16104.

62. Torrado, J. F.; González-Díaz, J. B.; González, M. U.; García-Martín, A.; and Armelles, G.,*Optics Express.* 2010, 15, 15635.

63. Temnov, V.V.; Armelles, G.; Woggon, U.; Guzatov, D.; Cebollada, A.; Garcia-Martin, A.; Garcia-Martin, J.; Thomay, T.; Leitenstorfer, A.; and Bratschitsch, R.,*Nature Photonics.* 2010, 4, 107.

64. (a) Kumah, D P; Cebollada, A; Clavero, C, Garc´ıa-Mart´ın,J R Skuza, J M, Lukaszew, R A; and Clarke1, R. *J. Phys. D: Appl. Phys.* 2007, 40, 2699 (b) Schouteden, K; and Van Haesendonck, C., *J. Phys.: Condens. Matter* 2010, 22, 255504.

65. Belotelov, V.I.; Doskolovich, L.L.; Zvezdin, A.K.,*Phys. Rev. Lett.* 2007, 98, 077401.

66. Johnson, C. J.; Dujardin, E.; Davis, S. A.; Murphy, C.J.; and Mann, S., *J. Mater. Chem.* 2002, 12, 1765.

67. Nikoobakht, B.; and El-Sayed, M. A., *Chem. Mater.* 2003, 15, 1957.

68. Handley, D. A. Colloidal Gold: properties, Methods, and Application; Academic Press: New York, 1989.

69. Lin, J.; Zhou, W.; Kumbhar, A.; Wiemann, J.; Fang, J.; Carpenter, E. E.; and O'Connor, C. J., *J. Solid State Chem.* 2001, 159, 26.

70. Bao, Y.; Calderon, H.; and Krishnan, K. M.,*J. Phys. Chem. C.* 2007, 111, 1941.

71. Cheng, G.; Walker, A. R. H.*J. Magnetism and Magnetic Mater.* 2007, 311, 31

72. Lyon, J. L.; Fleming, D. A.; Stone, M. B.; Schiffer, P.; and Williams, M. E.,*Nano Lett.* 2004, 4, 719

73. Templeton, A. C., Pietron, J. J., Murray, R. W., Mulvaney, P.,*J. Phys. Chem. B* 2000, 104, 564.

74. Girgis, E.; Khalil, W.K.B.; Emam, A.N.; Mohamed, M.B.; and Rao, K.V.,*Chem Research in Toxicology.* 2012, 25, 1086.

75. Ledo-Suárez, A.; Rivas, J.; Rodríguez-Abreu, C.F.; Rodríguez, M.J.; Pastor, E.; Hernández-Creus, A.; Oseroff, S. B.; López-Quintela, M.A.,*Angew Chem. Int. Ed.* 2007, 46, 8823.

76. Rodríguez-Vázquez, M.J.; Blanco, M.C.; Lourido, R.; Vázquez-Vázquez, C.; Pastor, E.; Planes, G.A.; Rivas, J.; López-Quintela, M.A.,*Langmuir.* 2008, 24, 12690.

77. Özkar, S.; and Finke, R.G. *Langmuir.* 2002, 18, 7653.

78. Reetz, M. T.; and Maase, M. *Advanced Materials*, 1999, 11, 773.

79. Link, S.; Mohamed, M. B.; and El-Sayed, M. A. *J. Phys. Chem. B* 1999, 103, 3073.

80. Boyer, P.; Ménard, D.; and Meunier, M.*J. Phys. Chem. C,* 2010, 114, 13497.

81. Xu, Z.; Hou, Y.; and Sun, S.*J. Am. Chem. Soc.*, 2007, 129, 8698.

82. Lica, G. C.; Zelakiewicz, B. S.; Constantinescu, M.; Tong, Y. Y. *J. Phys. Chem. B* 2004, 108, 19896.

83. Liu, M.; and Guyot-Sionnest, P. *J. Phys. Chem. B*, 2005, 109, 22192.

84. Khatri, H.; Packiaraj, G.; and Jotania, R. B. *Adv. Mater. Res.* 2014, 938, 14.

85. Shu-lai, W.E. N.; Jing-wei, C.; Hong, L.; Ying, L.; Xiu-chen, Z.; Yu-Feng, W.*J. Mater. Eng.*, 2014, 0(8), 21.

86. Crespo, P.; Litrán, R.; Rojas, T. C.; Multigner, M.; De la Fuente, J. M.; Sánchez-López, J. C.; Garcia, M. A.; Hernando, A.; Penadés, S.; and Fernández, A. *Phys. Rev.Let.*, 2004, 93, 087204.

RSC Advances

Insert Table of Contents artwork here